

Entanglement in a bright light source via Raman-driven coherence

Sajid Qamar,¹ M. Al-Amri,² and M. Suhail Zubairy^{1,3}

¹Centre for Quantum Physics, COMSATS Institute of Information and Technology, Islamabad, Pakistan

²The National Centre for Mathematics and Physics, KACST, P.O. Box 6086, Riyadh 11442, Saudi Arabia

³Department of Physics and Institute for Quantum Studies, Texas A&M University, College Station, Texas 77843-4242, USA

(Received 26 August 2008; published 30 January 2009)

We propose a two-photon correlated emission laser to generate entanglement amplifier for bright light source. The coherence between upper and lower levels is generated in a Raman-driven scheme using two external classical fields. The proposed scheme is practically more suitable for the macroscopic entanglement of photons of the two modes of the cavity field.

DOI: [10.1103/PhysRevA.79.013831](https://doi.org/10.1103/PhysRevA.79.013831)

PACS number(s): 42.50.Pq, 42.50.Dv, 42.65.Lm

According to the superposition principle, a quantum system may exist in a linear superposition of at least two different eigenstates of an observable. For a multipartite system, the corresponding superposition leads to quantum entanglement. The concept of entanglement is at the core of quantum computation, quantum communication, and quantum cryptography. Therefore, considerable effort has been devoted to the study of entangled states. More recently, studies have been made toward generating macroscopic entangled states of the objects [1].

We proposed a scheme for generating an optically macroscopic state of entangled state [2,3] in a correlated emission laser (CEL) [4–7]. The CEL-based scheme of a three-level atomic system in the cascade configuration uses coherence between the upper and the lower levels either to generate the phase-sensitive amplification [7–9] or to be used as an entanglement amplifier [2]. The required atomic coherence can be established using external driving fields. In [2], this is done by coupling the upper and the lower levels by a single driving field. As the coupling between the upper and the lower levels is dipole forbidden, this requires a higher-order process which is practically unsuitable.

To avoid this situation, certain schemes have been proposed for the two-photon phase-sensitive amplifier within the framework of multiwave mixing [9] and four-level Raman-driven system [10]. In the latter scheme the atomic coherence between upper and lower levels is established via a fourth level using two external classical driving fields.

We discuss here the question of generating macroscopic entanglement of photons in the two modes using a four-level Raman-driven system. The advantage is to get an experimentally more suitable driven system for the entanglement of bright light. We consider a four-level atomic medium placed inside a doubly resonant cavity as shown in Fig. 1. The atoms interact with the cavity modes resonantly. The coherence between the upper and the lower levels is introduced by driving the atoms with two external classical driving fields.

In order to ascertain the entanglement between the two cavity modes, we use a criterion which is based on quadrature measurements as given in [11] and known as Duan criterion. According to this criterion, a state of the system is entangled if the sum of the quantum fluctuations of two Einstein-Podolsky-Rosen operators \hat{u} and \hat{v} of the two modes satisfies the inequality

$$(\Delta\hat{u})^2 + (\Delta\hat{v})^2 < 2. \quad (1)$$

This is in general a sufficient condition for entanglement. For a Gaussian state, this is a sufficient as well as necessary condition. Here

$$\hat{u} = \hat{x}_1 + \hat{x}_2, \quad (2)$$

$$\hat{v} = \hat{p}_1 - \hat{p}_2, \quad (3)$$

and $\hat{x}_j = (a_j + a_j^\dagger)/\sqrt{2}$ and $\hat{p}_j = (a_j - a_j^\dagger)/\sqrt{2}i$ (with $j=1,2$) are the quadrature operators for the two modes 1 and 2 which can be measured using the balanced homodyne detection scheme [12]. On substituting the values of \hat{u} and \hat{v} to the left side of the Eq. (1), we obtain [13,14]

$$\begin{aligned} (\Delta\hat{u})^2 + (\Delta\hat{v})^2 = & 2(\langle a_1^\dagger a_1 \rangle + \langle a_2^\dagger a_2 \rangle + \langle a_1 a_2 \rangle + \langle a_1^\dagger a_2^\dagger \rangle - \langle a_1 \rangle \\ & \times \langle a_2 \rangle - \langle a_1^\dagger \rangle \langle a_2^\dagger \rangle + 1) - \langle a_1 \rangle \langle a_1^\dagger \rangle \\ & - \langle a_1^\dagger \rangle \langle a_1 \rangle - \langle a_2 \rangle \langle a_2^\dagger \rangle - \langle a_2^\dagger \rangle \langle a_2 \rangle. \end{aligned} \quad (4)$$

We need to calculate the corresponding moments in Eq. (4) to check for the entanglement generation. In the following, we develop a mathematical model for the entanglement amplifier.

Consider a four-level atom with energy levels $|a\rangle$, $|b\rangle$, $|c\rangle$, and $|d\rangle$ as shown in Fig. 1. The coherence between levels $|a\rangle$ and $|c\rangle$ is introduced via energy level $|d\rangle$ using two external classical driving fields with optical frequencies ν_1 and ν_2 . The atom interacts with the cavity modes having frequencies ν_3 and ν_4 inside a doubly resonant cavity. The interaction picture Hamiltonian of the system can be written as

$$\begin{aligned} \mathcal{H}_I(t) = & -\hbar \left[\frac{\Delta_1}{2} |a\rangle\langle a| - \frac{\Delta_2}{2} |c\rangle\langle c| + \frac{\Omega_1}{2} e^{i\varphi_1} |a\rangle\langle d| + \frac{\Omega_2}{2} e^{i\varphi_2} |c\rangle\langle d| \right. \\ & \left. \times \langle d| - g_1 a_1 |a\rangle\langle b| e^{i\Delta_1 t} - g_2 a_2 |b\rangle\langle c| e^{i\Delta_2 t} + \text{H.c.} \right], \end{aligned} \quad (5)$$

where a_1 (a_1^\dagger) and a_2 (a_2^\dagger) are the annihilation (creation) operators of the fields of frequencies ν_3 and ν_4 , whereas $\Delta_1 = \omega_d - \omega_a - \nu_1$ and $\Delta_2 = \nu_2 - \omega_d + \omega_c$ are the detunings corresponding to the classical driving fields of frequencies ν_1 and ν_2 , respectively.

The master equation of the system in the configuration in Fig. 1(b) can be obtained via standard method of the laser

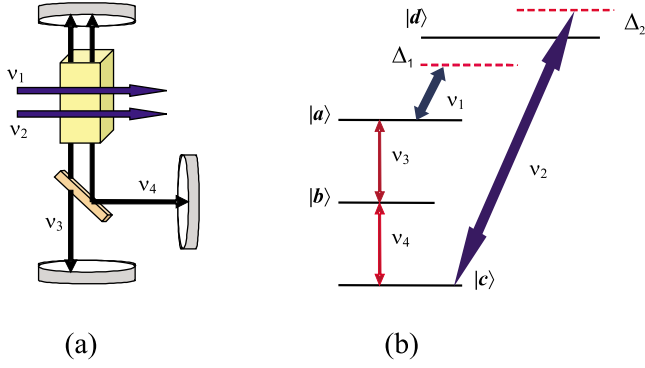


FIG. 1. (Color online) (a) Atomic medium inside a doubly resonant cavity; two external classical driving fields are applied. (b) Four-level atomic configuration: The transitions between $|a\rangle \rightarrow |b\rangle$ and $|b\rangle \rightarrow |c\rangle$ are resonant with the cavity field with frequencies ν_3 and ν_4 . The coherence between atomic levels $|a\rangle$ and $|c\rangle$ is established via off-resonant transitions $|a\rangle \leftrightarrow |d\rangle$ and $|c\rangle \leftrightarrow |d\rangle$ using external driving fields at frequencies ν_1 and ν_2 . The corresponding detunings are $\Delta_1 = \omega_{da} - \nu_1$ and $\Delta_2 = \nu_2 - \omega_{dc}$.

theory. Here we only consider the linear amplification of the signal field which is sufficient for the discussion of entanglement generation [2,13,14]. Therefore, we consider a quantum-mechanical treatment for the transitions between levels $|a\rangle$ and $|b\rangle$ and $|b\rangle$ and $|c\rangle$ up to the second order in the coupling constants g_1 and g_2 . However, for strong driving fields, we consider all orders in the Rabi frequencies Ω_1 and Ω_2 . We also assume that the atoms are injected in the cavity in level $|d\rangle$ at a rate r and the resonance condition $\Delta_1 + \Delta_2 = 0$ is satisfied. The resulting equation for the reduced density operator for the required cavity field modes is therefore written as

$$\begin{aligned} \dot{\rho} = & -[B_{11}^* a_1 a_1^\dagger \rho + B_{11} \rho a_1 a_1^\dagger - (B_{11} + B_{11}^*) a_1^\dagger \rho a_1 + B_{22}^* a_2^\dagger a_2 \rho \\ & + B_{22} \rho a_2^\dagger a_2 - (B_{22} + B_{22}^*) a_2 \rho a_2^\dagger + B_{12}^* a_1 a_2 \rho + B_{21} \rho a_1 a_2 \\ & - (B_{12}^* + B_{21}) a_2 \rho a_1 - (B_{12} + B_{21}^*) a_1^\dagger \rho a_2^\dagger + B_{12} \rho a_2^\dagger a_1^\dagger \\ & + B_{21}^* a_2^\dagger a_1^\dagger \rho] - \kappa_1 (a_1^\dagger a_1 \rho - 2a_1 \rho a_1^\dagger + \rho a_1^\dagger a_1) \\ & - \kappa_2 (a_2^\dagger a_2 \rho - 2a_2 \rho a_2^\dagger + \rho a_2^\dagger a_2), \end{aligned} \quad (6)$$

where κ_1 and κ_2 are the cavity decay rates of mode 1 and mode 2, respectively. A detailed procedure for this derivation is presented in [10]. The coefficients in Eq. (6) for the case where $\Delta_1 = -\Delta_2 = 0$ are calculated as

$$B_{11} = \frac{6g_1^2 r \gamma^2 \Omega_1^2}{D}, \quad (7)$$

$$B_{22} = \frac{6g_2^2 r \gamma^2 \Omega_2^2}{D}, \quad (8)$$

$$B_{12} = \frac{6g_1 g_2 r \gamma^2 \Omega_1 \Omega_2}{D} e^{i(\varphi_1 - \varphi_2)}, \quad (9)$$

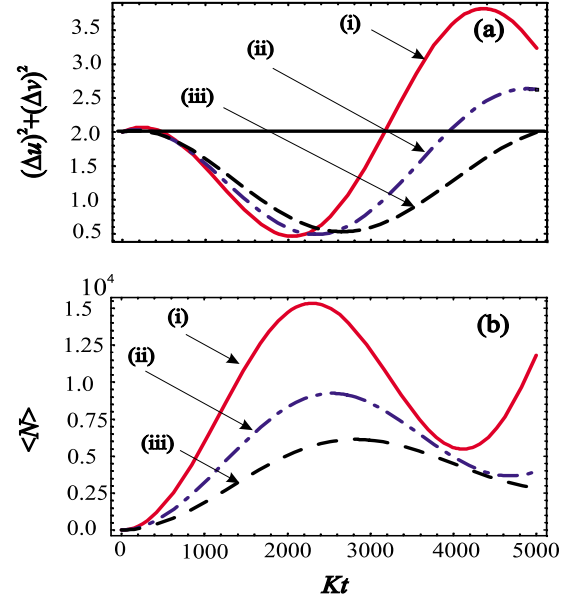


FIG. 2. (Color online) Resonant case: time evolutions of (a) $(\Delta \hat{u})^2 + (\Delta \hat{v})^2$ and (b) $\langle N \rangle = \langle a_1^\dagger a_1 \rangle + \langle a_2^\dagger a_2 \rangle$ for initial vacuum state (in terms of normalized time Kt , where $K = g^2 r / \gamma^2$). Different parameters are selected as $r = 50$ MHz, $\kappa_1 \approx \kappa_2 = 0.05$ MHz, $\gamma = 20$ MHz, and $\Omega_1 \approx \Omega_2 =$ (i) 40, (ii) 50, and (iii) 60 MHz.

$$B_{21} = \frac{6g_1 g_2 r \gamma^2 \Omega_1 \Omega_2}{D} e^{-i(\varphi_1 - \varphi_2)}, \quad (10)$$

where $D = 2\gamma^2(4\gamma^2 + \Omega_1^2 + \Omega_2^2)(\gamma^2 + \Omega_1^2 + \Omega_2^2)$ and γ is the atomic decay rate from levels $|a\rangle$, $|c\rangle$, and $|d\rangle$, which for simplicity's sake we assume to be equal. Here B_{11} is the gain term for the first mode and B_{22} is the absorption term for the second mode. We observe from Eqs. (7) and (8) that the system does not behave as parametric oscillator because B_{11} and B_{22} never go to zero for the condition $\Omega_1, \Omega_2 \gg \gamma$ [10].

The equations of motion for the various moments in Eq. (4) are required to verify the entanglement generation. These can easily be obtained from Eq. (6) by taking traces for the corresponding moments. For the choice $\varphi_1 - \varphi_2 = 0$, we get two sets of coupled rate equations,

$$\frac{d}{dt} \langle a_1^\dagger a_1 \rangle = 2(B_{11} - \kappa_1) \langle a_1^\dagger a_1 \rangle + B_{12} (\langle a_1 a_2 \rangle + \langle a_1^\dagger a_2^\dagger \rangle) + 2B_{11}, \quad (11)$$

$$\begin{aligned} \frac{d}{dt} (\langle a_1 a_2 \rangle + \langle a_1^\dagger a_2^\dagger \rangle) = & (B_{11} - B_{22} - \kappa_1 - \kappa_2) (\langle a_1 a_2 \rangle + \langle a_1^\dagger a_2^\dagger \rangle) \\ & + 2B_{12} \langle a_2^\dagger a_2 \rangle - 2B_{21} \langle a_1^\dagger a_1 \rangle - 2B_{21}, \end{aligned} \quad (12)$$

$$\frac{d}{dt} \langle a_2^\dagger a_2 \rangle = -2(B_{22} + \kappa_2) \langle a_2^\dagger a_2 \rangle - B_{21} (\langle a_1 a_2 \rangle + \langle a_1^\dagger a_2^\dagger \rangle), \quad (13)$$

$$\frac{d}{dt}\langle a_1 \rangle = (B_{11} - \kappa_1)\langle a_1 \rangle + B_{12}\langle a_2^\dagger \rangle, \quad (14)$$

$$\frac{d}{dt}\langle a_2^\dagger \rangle = -(B_{22} + \kappa_2)\langle a_2^\dagger \rangle - B_{21}\langle a_1 \rangle. \quad (15)$$

The time evolution of the various moments can be deter-

mined and analytic expressions can be obtained for an arbitrary choice of initial state. These can then be used to test entanglement criterion (4) and calculate the mean photon number $\langle N \rangle$. However, the resulting expressions are cumbersome and complex to reproduce here. Hence we present exact solutions of $(\Delta\hat{u})^2 + (\Delta\hat{v})^2$ and $\langle N \rangle = \langle a_1^\dagger a_1 \rangle + \langle a_2^\dagger a_2 \rangle$ for an initial vacuum state for the two modes only,

$$\begin{aligned} [(\Delta\hat{u})^2 + (\Delta\hat{v})^2]_t &= \frac{2\alpha_3}{\alpha_1} e^{\alpha_1 t/2} \sinh \frac{\alpha_1 t}{2} - \alpha_2 \beta_1 \alpha_3 \left[\frac{(\alpha_1 + \eta_2) e^{\alpha_1 t}}{\alpha_1 \prod_i (\alpha_1 - \lambda_i)} + \frac{\eta_2}{\alpha_1 \prod_i \lambda_i} - \sum_{i,j,k,i \neq j, j \neq k} \frac{e^{\lambda_i t} (\eta_2 + \lambda_i)}{\lambda_i (\alpha_1 - \lambda_i) (\lambda_i - \lambda_j) (\lambda_i - \lambda_k)} \right] \\ &+ \alpha_2 \beta_4 \left[\frac{\eta_2}{\prod_i \lambda_i} - \sum_{i,j,k,i \neq j, j \neq k} \frac{e^{\lambda_i t} (\eta_2 + \lambda_i)}{\lambda_i (\lambda_i - \lambda_j) (\lambda_i - \lambda_k)} \right] + \eta_2 \left[\sum_{i,j,k,i \neq j, j \neq k} \frac{e^{\lambda_i t} (\lambda_i - \alpha_1)}{\lambda_i (\lambda_i - \lambda_j) (\lambda_i - \lambda_k)} \right] \\ &+ \eta_1 \beta_4 \left[\sum_{i,j,k,i \neq j, j \neq k} \frac{e^{\lambda_i t} (\lambda_i - \alpha_1)}{\lambda_i (\lambda_i - \lambda_j) (\lambda_i - \lambda_k)} + \frac{\alpha_1}{\prod_i \lambda_i} \right] - \beta_1 \alpha_3 \left[\sum_{i,j,k,i \neq j, j \neq k} \frac{e^{\lambda_i t} (\eta_2 + \lambda_i)}{\lambda_i (\lambda_i - \lambda_j) (\lambda_i - \lambda_k)} - \frac{\eta_2}{\prod_i \lambda_i} \right] \\ &- \beta_4 \left[\sum_{i,j,k,i \neq j, j \neq k} \frac{e^{\lambda_i t} (\lambda_i - \alpha_1)}{(\lambda_i - \lambda_j) (\lambda_i - \lambda_k)} + \frac{\eta_2 \alpha_1}{\prod_i \lambda_i} \right] + \eta_1 \beta_1 \alpha_3 \left[\sum_{i,j,k,i \neq j, j \neq k} \frac{e^{\lambda_i t}}{\lambda_i (\lambda_i - \lambda_j) (\lambda_i - \lambda_k)} - \frac{1}{\prod_i \lambda_i} \right], \end{aligned} \quad (16)$$

$$\begin{aligned} \langle N \rangle_t &= \frac{2\alpha_3}{\alpha_1} e^{\alpha_1 t/2} \sinh \frac{\alpha_1 t}{2} - \alpha_2 \beta_1 \alpha_3 \left[\frac{(\alpha_1 + \eta_2) e^{\alpha_1 t}}{\alpha_1 \prod_i (\alpha_1 - \lambda_i)} + \frac{\eta_2}{\prod_i \lambda_i} - \sum_{i,j,k,i \neq j, j \neq k} \frac{e^{\lambda_i t}}{(\alpha_1 - \lambda_i) (\lambda_i - \lambda_j) (\lambda_i - \lambda_k)} \right] \\ &+ \alpha_2 \beta_4 \left[\sum_{i,j,k,i \neq j, j \neq k} \frac{e^{\lambda_i t} (\eta_2 + \lambda_i)}{\lambda_i (\lambda_i - \lambda_j) (\lambda_i - \lambda_k)} \right] + \eta_2 \beta_1 \alpha_3 \left[\sum_{i,j,k,i \neq j, j \neq k} \frac{e^{\lambda_i t}}{\lambda_i (\lambda_i - \lambda_j) (\lambda_i - \lambda_k)} \right] \\ &+ \eta_1 \beta_4 \left[\sum_{i,j,k,i \neq j, j \neq k} \frac{e^{\lambda_i t} (\lambda_i - \alpha_1)}{\lambda_i (\lambda_i - \lambda_j) (\lambda_i - \lambda_k)} \right]. \end{aligned} \quad (17)$$

Here,

$$\alpha_1 = 2(B_{11} - \kappa_1), \quad (18)$$

$$\alpha_2 = B_{12}, \quad (19)$$

$$\alpha_3 = 2B_{11}, \quad (20)$$

$$\beta_1 = 2B_{21}, \quad (21)$$

$$\beta_2 = B_{11} - B_{22} - (\kappa_1 + \kappa_2), \quad (22)$$

$$\beta_3 = 2B_{12}, \quad (23)$$

$$\beta_4 = 2B_{21}, \quad (24)$$

$$\eta_1 = B_{21}, \quad (25)$$

$$\eta_2 = 2(B_{22} + \kappa_2). \quad (26)$$

λ_i 's are the roots of the cubic equation,

$$\lambda^3 + a\lambda^2 + b\lambda + c = 0, \quad (27)$$

where

$$a = \eta_2 - \alpha_1 - \beta_2, \quad (28)$$

$$b = -\alpha_1 \eta_2 + \beta_1 \alpha_2 - \alpha_2 \eta_2 + \alpha_1 \beta_2 + \beta_3 \eta_1, \quad (29)$$

$$c = \beta_1 \alpha_2 \eta_2 + \alpha_1 \beta_2 \eta_2 - \alpha_1 \beta_3 \eta_1. \quad (30)$$

We observe from rate equations (11) and (13) that α_1 [Eq. (18)] and η_2 [Eq. (26)] must be positive in order to maintain the mean number of photons growing in the two modes

which is required for the entanglement generation in our suggested system.

We know from our earlier work [15] that the characteristic function of the two-mode field in the Wigner function representation is defined as

$$\chi(\zeta_1, \zeta_2, t) = (e^{(B_{11}-\kappa_1)\zeta_1(\partial/\partial\zeta_1)-(B_{22}+\kappa_2)\zeta_2(\partial/\partial\zeta_2)-B_{12}\zeta_2^*(\partial/\partial\zeta_1)+B_{21}\zeta_1^*(\partial/\partial\zeta_2)-[(B_{11}+\kappa_1)/2]\zeta_1^*\zeta_1-[(B_{22}+\kappa_2)/2]\zeta_2^*\zeta_2+[(B_{12}^*+B_{21}^*)/2]\zeta_1\zeta_2+c.c.})\chi(\zeta_1, \zeta_2, 0). \quad (32)$$

Equation (32) can be solved exactly by defining a set of operators which form a closed Lie algebra and using the operator-ordering theorem. We assume that the two-mode field is initially in a two-mode Gaussian state having a characteristic function [16]

$$\chi(\zeta_1, \zeta_2, 0) = e^{-(1/2)\zeta V_0 \zeta^\dagger}, \quad (33)$$

with $\zeta = (\zeta_1^*, \zeta_1, \zeta_2^*, \zeta_2)$ and

$$V_0 = \begin{pmatrix} n_1 & m_1 & m_s & m_c \\ m_1^* & n_1 & m_c^* & m_s^* \\ m_s^* & m_c & n_2 & m_2 \\ m_c^* & m_s & m_2^* & n_2 \end{pmatrix}, \quad (34)$$

where V_0 is the covariance matrix, $n_i = \langle a_i^\dagger a_i \rangle + 1/2$, $m_i = -\langle a_i^2 \rangle$ (with $i=1,2$), $m_c = -\langle a_1 a_2 \rangle$, and $m_s = \langle a_1 a_2^\dagger \rangle$. Hence we get the time-dependent solution of Eq. (32) as

$$\chi(\zeta_1, \zeta_2, t) = e^{-(1/2)\zeta V_t \zeta^\dagger}, \quad (35)$$

where

$$V_t = \begin{pmatrix} h_1 & h_{11}^* & h_{12}^* & h_3^* \\ h_{11} & h_1 & h_3 & h_{12} \\ h_{12} & h_3^* & h_2 & h_{22}^* \\ h_3 & h_{12}^* & h_{22} & h_2 \end{pmatrix}, \quad (36)$$

and the elements of V_t are given in the Appendix. The result shows that the two-mode field state at time t evolves in a two-mode Gaussian state if it is initially in a two-mode Gaussian state. The entanglement property of the two-mode Gaussian state with covariance matrix (36) can be analyzed by the use of two sufficient and necessary separability criteria for the two-mode Gaussian state [11,17].

We now discuss how the proposed CEL with Raman-driven coherence serves as a source of macroscopic entanglement of the light. We assume that the cavity modes are resonant with the atomic transitions $|a\rangle \leftrightarrow |b\rangle$ and $|b\rangle \leftrightarrow |c\rangle$. However, in the case of external fields, we consider resonant as well as off-resonant interaction. The analysis for the resonant case is presented in Figs. 2 and 3, whereas for the off-resonant case the results are presented in Figs. 4 and 5. Here we would like to mention that the time evolutions of the

$$\chi(\zeta_1, \zeta_2, t) = \text{Tr}[\rho(t) e^{\zeta_1^\dagger a_1^\dagger - \zeta_1^* a_1} e^{\zeta_2^\dagger a_2^\dagger - \zeta_2^* a_2}]. \quad (31)$$

Therefore, the general solution for master equation (6) can also be obtained by using the characteristic function $\chi(\zeta_1, \zeta_2, t)$, which for two-mode field under consideration is given by

required quantities $(\Delta\hat{u})^2 + (\Delta\hat{v})^2$ and mean photon number $\langle N \rangle = \langle a_1^\dagger a_1 \rangle + \langle a_2^\dagger a_2 \rangle$ are plotted versus dimensionless quantity Kt , where the parameter $K = g^2 r / \gamma^2$. Also in all the numerical results we use the dimensionless parameters Ω_1 / γ , Ω_2 / γ , Δ_1 / γ , and Δ_2 / γ .

For the resonant case, the two external classical driving fields, having Rabi frequencies Ω_1 and Ω_2 , are resonant with the atomic transitions $|a\rangle \leftrightarrow |d\rangle$ and $|c\rangle \leftrightarrow |d\rangle$, which means $\Delta_1 = -\Delta_2 = 0$. We plot the time developments of $(\Delta\hat{u})^2 + (\Delta\hat{v})^2$ and mean photon number $\langle N \rangle = \langle a_1^\dagger a_1 \rangle + \langle a_2^\dagger a_2 \rangle$ in Figs. 2(a) and 2(b), respectively, for an initial vacuum state. As time increases, the value of $(\Delta\hat{u})^2 + (\Delta\hat{v})^2$ becomes less than 2 and it remains less than 2 for some time. This shows that the proposed Raman-driven system behaves as an entanglement amplifier of photons of the two cavity modes. This is due to the coherence introduced between the upper and lower levels of the atom which is controlled by the two external driving fields' Rabi frequencies. We observe that for

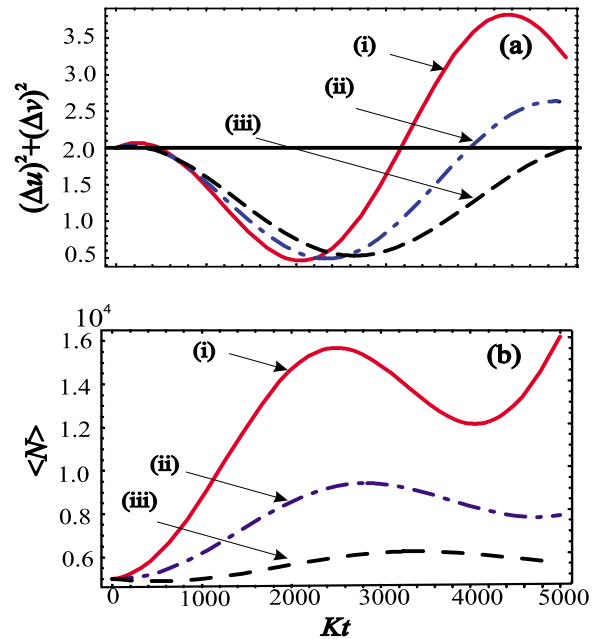


FIG. 3. (Color online) Resonant case: time evolutions of (a) $(\Delta\hat{u})^2 + (\Delta\hat{v})^2$ and (b) $\langle N \rangle = \langle a_1^\dagger a_1 \rangle + \langle a_2^\dagger a_2 \rangle$ for initial coherent state $|50, -50\rangle$. The rest of the parameters are the same as in Fig. 2.

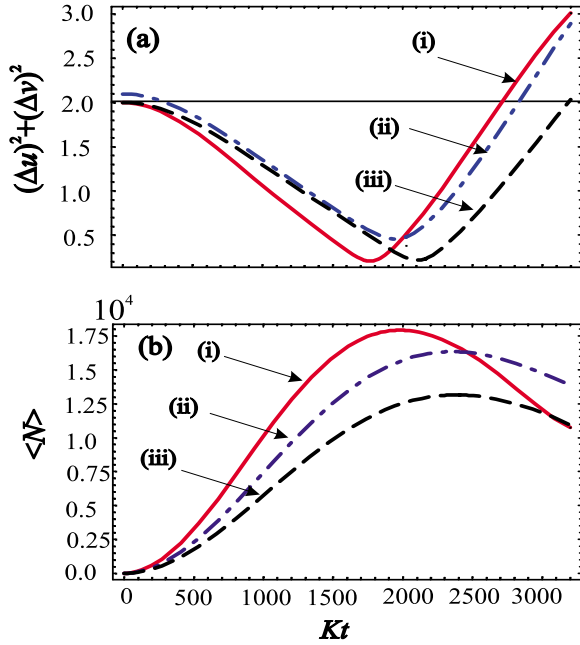


FIG. 4. (Color online) Off-resonant case: time evolutions of (a) $(\Delta\hat{u})^2 + (\Delta\hat{v})^2$ and (b) $\langle N \rangle = \langle a_1^\dagger a_1 \rangle + \langle a_2^\dagger a_2 \rangle$ for initial vacuum state. Here $\Omega_1 \approx \Omega_2 = 40$ MHz and $\Delta_1 = -\Delta_2 =$ (i) 15, (ii) 20, and (iii) 25 MHz. The other parameters are same as in Fig. 2.

the higher values of the Rabi frequencies (where $\Omega_1 \approx \Omega_2$) the period of entanglement increases considerably. For example, when $\Omega_1 \approx \Omega_2 = 40$ MHz the entanglement starts at $Kt \approx 500$ and ends at $Kt \approx 3000$. The entanglement period increases to $Kt \approx 500 - 5000$ when $\Omega_1 \approx \Omega_2 = 60$ MHz [Fig. 2(a)]. Figure 2(b) shows the behavior of mean photon number $\langle N \rangle$ as time evolves. The mean photon number having initial value 0 at the beginning ($Kt=0$) builds up significantly during the time of entanglement. As observed analytically, it is found numerically as well that the values of $\alpha_1 = 2(B_{11} - \kappa_1)$ and $\eta_2 = 2(B_{22} + \kappa_2)$ remained > 0 in our results.

In Fig. 3, we do the same analysis as done in Fig. 2. However, the cavity modes are now considered to be in initial coherent state $|50, -50\rangle$. The results show a similar behavior, as has been observed for the initial vacuum state, of the time evolution of the two quantities. However, the mean photon number $\langle N \rangle = \langle a_1^\dagger a_1 \rangle + \langle a_2^\dagger a_2 \rangle$ is a bit higher now. This is due to the fact that for initial coherent state $|50, -50\rangle$ the mean photon number at $Kt=0$ is 2500.

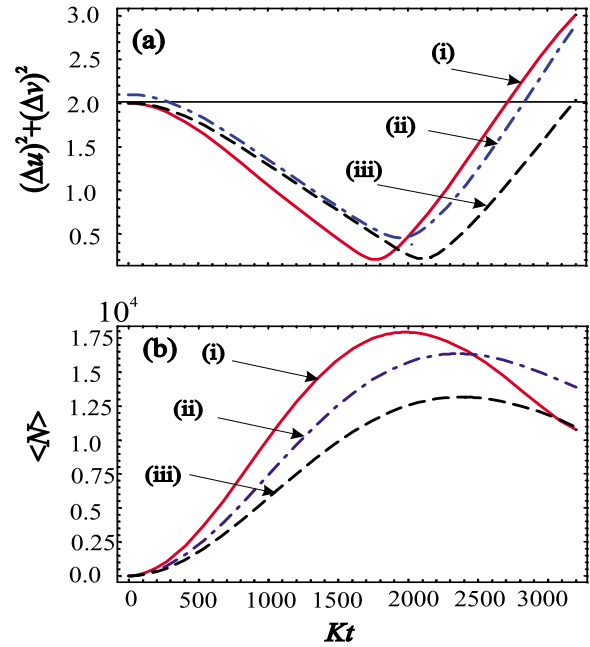


FIG. 5. (Color online) Off-resonant case: time evolutions of (a) $(\Delta\hat{u})^2 + (\Delta\hat{v})^2$ and (b) $\langle N \rangle = \langle a_1^\dagger a_1 \rangle + \langle a_2^\dagger a_2 \rangle$ for initial coherent state $|50, -50\rangle$. The other parameters are the same as in Fig. 4.

From Figs. 2(b) and 3(b), we also observe that the value of the mean photon number depends on the strength of the driving fields and the maximum value decreases with increasing Rabi frequencies amplitudes. This is due to the presence of the cavity losses κ_1 and κ_2 which determine the threshold condition for Ω_1 and Ω_2 . Here, the threshold condition is found to be $\Omega_1 = \Omega_2 \approx 10$ MHz.

Next, we consider the driving fields to be off-resonant with the respective atomic transitions. However, they follow the resonance condition given by $\Delta_1 + \Delta_2 = 0$. For simplicity, we use $\Delta = \Delta_1 = -\Delta_2$ and analyze the macroscopic entanglement generation and mean photon number for different choices of the detuning Δ . We would like to mention that the analytical computations for off-resonant case become rather complex when we consider $\Omega_1 \neq \Omega_2$ which has been considered in deriving expressions (7)–(10). Therefore, keeping in mind the selection of parameters in the resonant case and the results which we have observed earlier, it is reasonable to consider that $\Omega_1 = \Omega_2 = \Omega$ along with $\varphi_1 = \varphi_2 = \varphi$. Under these assumptions, all the coefficients B_{nm} ($n, m = 1, 2$) in Eq. (6) become equal,

$$B_{nm} = g^2 r \frac{-2(\gamma - i\Delta)\Delta\Omega e^{-i\varphi} + (3\gamma + i\Delta)\Omega^2}{4\gamma(\gamma^2 + \Delta^2 + 2\Omega^2)(\gamma^2 + 2i\gamma\Delta + \Delta^2) + \Omega^2 - 4\Delta\Omega \cos(\varphi)}, \quad (37)$$

where $n, m = 1, 2$.

The effect of atom field detuning Δ on the entanglement amplifier and mean photon number is presented in Figs. 4 and 5. We again plot the time evolutions of the Duan crite-

on $(\Delta\hat{u})^2 + (\Delta\hat{v})^2$ and mean photon number $\langle N \rangle$ for the initial vacuum state in Fig. 4 and for the initial coherent state $|50, -50\rangle$ in Fig. 5. In each case, the system becomes a source of macroscopic entanglement of bright light. The pe-

riod of entanglement increases while the mean photon number $\langle N \rangle$ decreases with increasing detuning Δ . We note that the threshold condition changes and it becomes $\Omega \approx 45, 55,$ and 65 MHz for $\Delta = 15, 20,$ and 25 MHz, respectively. Here, it should be noted that these threshold conditions are calculated numerically for resonant as well as off-resonant cases.

It is already mentioned that levels $|a\rangle, |c\rangle,$ and $|d\rangle$ decay with a common rate γ to some other atomic levels. These atomic decays do not affect the entanglement generation unless we are working near threshold conditions. Further, we do not consider transverse decay rates in the system whose nonvanishing values decreases the degree of coherence between atomic levels $|a\rangle$ and $|c\rangle$. We know from our earlier work that phase diffusion of the pump field reduces the entanglement in a nondegenerate parametric amplifier [18] and in a correlated spontaneous emission laser [13]. Therefore, we expect a similar reduction in macroscopic entanglement in our proposed system as well. The choices of parameters in all these results correspond to the experimental parameters quoted in [2] and references therein.

In conclusion, we have proposed a CEL-based Raman-driven four-level atomic scheme to generate macroscopic entanglement of light. The atomic coherence is introduced using two external classical driving fields. The bright light entanglement is generated in the resonant as well as off-resonant interaction of the atom with the external driving

fields. It is observed that the entanglement is independent of the initial state of the cavity modes. The advantage of this proposed entanglement amplifier over its predecessors is twofold. First, the atomic coherence is introduced through Raman-driven setup and, second, there is no dipole-forbidden transition involved. This makes the system practically more suitable. It is also observed that the system does not behave as parametric oscillator because B_{11} and B_{22} , which correspond to the emission from level $|a\rangle$ and absorption to level $|c\rangle$, never go to zero for the condition $\Omega_1, \Omega_2 \gg \gamma$. The scheme may be implemented experimentally by placing an atomic medium, having four-level atoms, inside the doubly resonant cavity. The atomic medium is prepared in the initial state $|d\rangle$ by incoherent pumping, whereas the coherence between levels $|a\rangle$ and $|c\rangle$ is introduced via level $|d\rangle$ using two coherent external classical fields. Also as an alternative approach, the initially prepared atoms having long-lived state may pass through the doubly resonant cavity one at a time. During the passage, atom interacts with the external coherent classical fields and hence introduce atomic coherence between upper and lower levels [19,20]. Here, we would like to mention that for appropriate conditions the proposed atomic system is equivalent to the injected coherence system [7] and never reduces to the one studied in [8] and [9]. For a detailed analysis, see [10].

We thank Shahid Qamar for some enlightened discussion on the subject. This research was supported in part by grants from King Abdulaziz City for Science and Technology (KACST) and the Qatar National Research Fund (QNRF). M.S.Z. is grateful to the Alexander von Humboldt Foundation for supporting this work. The authors would also like to thank COMSTECH for their support.

APPENDIX

Here we present the elements of V_s , which appear in Eq. (36).

$$\begin{aligned}
 h_1 &= \frac{n_1 \omega_1^4 + 4n_2 B_{21}^2 \omega_1^2 \sinh^2(dt/2) - 2B_{21} \omega_1^3 \sinh(dt/2)(m_c^* - \text{c.c.})}{d^2 \omega_1^2} f - f_1, \\
 h_2 &= \frac{n_1 B_{12}^2 \omega_1^2 \sinh^2(dt/2) + n_2 d^2 \omega_2^2 - 2B_{12} \omega_1 \omega_2^2 \sinh(dt/2)(m_c^* - \text{c.c.})}{d^2 \omega_1^2} f - f_2, \\
 h_{11} &= \frac{m_1^* \omega_1^4 - 4m_2 B_{21}^2 \omega_1^2 \sinh^2(dt/2) + 4m_s^* B_{21} \omega_1^3 \sinh(dt/2)}{d^2 \omega_1^2} f, \\
 h_{22} &= \frac{-4m_1 B_{12}^2 \omega_1^2 \sinh^2(dt/2) + 4m_s B_{12} \omega_1 \omega_2^2 \sinh(dt/2) + m_2^* \omega_2^4}{d^2 \omega_1^2} f, \\
 h_{12} &= \frac{-2m_1^* B_{12} \omega_1^2 \sinh(dt/2) + 2m_2 B_{21} \omega_2^2 \sinh(dt/2) + m_s^* (2\omega_2^2 - d^2)}{d^2 \omega_1^2} f, \\
 h_3 &= \frac{2n_1 B_{12} \omega_1^3 \sinh(dt/2) + 2n_2 B_{21} \omega_1 \omega_2^2 \sinh(dt/2) + m_c^* \omega_1^2 \omega_2^2 - m_c \omega_1 (\omega_2^2 - d^2)}{d^2 \omega_1^2} f - f_3^*,
 \end{aligned}$$

$$f_i = \frac{1}{2d^2} [C_{i1}(fe^{dt} - 1) - C_{i2}(fe^{-dt} - 1)] + \frac{C_{i3}}{2d^2}(f - 1), \quad i = 1, 2, 3,$$

$$C_{11(2)} = \frac{[b_1d \pm (B_{21}^2 - B_{12}B_{21})](\alpha_1 + \eta_2 \pm 2d) \pm 4(B_{21}^2b_2 - B_{12}B_{21}b_1)}{\alpha_1 - \eta_2 \pm 2d},$$

$$C_{1(2)3} = \frac{2(B_{12}B_{21} - B_{21}^2)(\alpha_1 + \eta_2) \pm 8B_{21(12)}(B_{12}b_1 - B_{21}b_2)}{\alpha_1 - \eta_2},$$

$$C_{21(2)} = \frac{[b_2d \pm (B_{12}^2 - B_{12}B_{21})](- \eta_2 - \alpha_1 \pm 2d) \pm 4(B_{12}^2b_1 - B_{12}B_{21}b_2)}{\alpha_1 - \eta_2 \pm 2d},$$

$$C_{31(2)} = \frac{\pm 4B_{12}B_{21}(B_{12} - B_{21}) \mp B_{12}b_1(\alpha_1 + \eta_2 \pm 2d) \pm 2b_2B_{21}(\alpha_1 - \alpha_2 \mp d)}{\alpha_1 - \eta_2 \pm 2d},$$

$$C_{33} = \frac{(B_{12} - B_{21})(\alpha_1 + \eta_2)^2 + 4(B_{12}b_1 - B_{21}b_2)(\alpha_1 + \eta_2)}{\alpha_1 - \eta_2},$$

$$f = e^{(\alpha_1 - \eta_2)t/2}, \quad \omega_1 = d \cosh(dt/2) + \frac{(\alpha_1 + \eta_2)}{2} \sinh(dt/2), \quad \omega_2 = \sqrt{\omega_1^2 + 4B_{12}B_{21} \sinh(dt/2)}, \alpha_1 = 2(B_{11} - \kappa_1),$$

$$\eta_2 = -2b_2 = 2(B_{22} + \kappa_2), \quad d = \frac{\sqrt{(\alpha_1 + \eta_2)^2 + 16B_{12}B_{21}}}{2}, \quad b_1 = -B_{11} - \kappa_1.$$

-
- [1] A. Furusawa, J. L. Sorensen, S. L. Braunstein, C. A. Fuchs, H. J. Kimble, and E. S. Polzik, *Science* **282**, 706 (1998); B. Julsgaard, A. Kozhekin, and E. S. Polzik, *Nature (London)* **413**, 400 (2001); W. P. Bowen, N. Treps, R. Schnabel, and P. K. Lam, *Phys. Rev. Lett.* **89**, 253601 (2002); C. Simon and D. Bouwmeester, *ibid.* **91**, 053601 (2003).
- [2] H. Xiong, M. O. Scully, and M. S. Zubairy, *Phys. Rev. Lett.* **94**, 023601 (2005), and references therein.
- [3] L. Zhou, H. Xiong, and M. S. Zubairy, *Phys. Rev. A* **74**, 022321 (2006).
- [4] M. O. Scully, *Phys. Rev. Lett.* **55**, 2802 (1985); M. O. Scully and M. S. Zubairy, *Phys. Rev. A* **35**, 752 (1987).
- [5] M. O. Scully and M. S. Zubairy, *Quantum Optics* (Cambridge University Press, Cambridge, England, 1997).
- [6] M. O. Scully, K. Wodkiewicz, M. S. Zubairy, J. Bergou, N. Lu, and J. Meyer ter Vehn, *Phys. Rev. Lett.* **60**, 1832 (1988); J. Bergou, M. Orszag, and M. O. Scully, *Phys. Rev. A* **38**, 768 (1988); K. Zaheer and M. S. Zubairy, *ibid.* **38**, 5227 (1988); N. A. Ansari and M. S. Zubairy, *ibid.* **40**, 5690 (1989); C. A. Blockley and D. F. Walls, *ibid.* **43**, 5049 (1991); M. Majeed and M. S. Zubairy, *ibid.* **44**, 4688 (1991); U. W. Rathe and M. O. Scully, *ibid.* **52**, 3193 (1995).
- [7] M. O. Scully and M. S. Zubairy, *Opt. Commun.* **66**, 303 (1988).
- [8] N. A. Ansari, J. Gea-Banacloche, and M. S. Zubairy, *Phys. Rev. A* **41**, 5179 (1990).
- [9] N. A. Ansari, *Phys. Rev. A* **46**, 1560 (1992); Y.-X. Ping, B. Zhang, and Z. Cheng, *Eur. Phys. J. D* **44**, 175 (2007).
- [10] S. Qamar, S.-Y. Zhu, and M. S. Zubairy, *Opt. Commun.* **147**, 274 (1998).
- [11] L.-M. Duan, G. Giedke, J. I. Cirac, and P. Zoller, *Phys. Rev. Lett.* **84**, 2722 (2000).
- [12] H. P. Yuen and J. H. Shapiro, *IEEE Trans. Inf. Theory* **26**, 78 (1980).
- [13] S. Qamar, H. Xiong, and M. S. Zubairy, *Phys. Rev. A* **75**, 062305 (2007).
- [14] S. Qamar, F. Ghafoor, M. Hillery, and M. S. Zubairy, *Phys. Rev. A* **77**, 062308 (2008).
- [15] H.-T. Tan, S.-Y. Zhu, and M. S. Zubairy, *Phys. Rev. A* **72**, 022305 (2005).
- [16] B.-G. Englert and K. Wódkiewicz, *Phys. Rev. A* **65**, 054303 (2002).
- [17] R. Simon, *Phys. Rev. Lett.* **84**, 2726 (2000).
- [18] K. Ahmed, H. Xiong, and M. S. Zubairy, *Opt. Commun.* **262**, 129 (2006).
- [19] D. Meschede, H. Walther, and G. Müller, *Phys. Rev. Lett.* **54**, 551 (1985).
- [20] J. M. Raimond, M. Brune, and S. Haroche, *Rev. Mod. Phys.* **73**, 565 (2001).